Dual roles of borax in kinetics of calcium sulfate dihydrate formation

ARTICLE *in* LANGMUIR · MAY 2007

Impact Factor: 4.38 · DOI: 10.1021/la062366g · Source: PubMed

5 AUTHORS, INCLUDING:

Haihua Pan
Zhejiang University
65 PUBLICATIONS **1,046** CITATIONS
SEE PROFILE

Jinhui Tao
Pacific Northwest National Laboratory
36 PUBLICATIONS **626** CITATIONS
SEE PROFILE

X. R. Xu
Zhejiang University
67 PUBLICATIONS **1,059** CITATIONS
SEE PROFILE

Ruikang Tang
Zhejiang University
119 PUBLICATIONS **2,209** CITATIONS
SEE PROFILE

Dual Roles of Borax in Kinetics of Calcium Sulfate Dihydrate Formation

Wenge Jiang,[†] Haihua Pan,[†,‡] Jinhui Tao,[†] Xurong Xu,[†,‡] and Ruikang Tang*,[†,‡]

Department of Chemistry and Research Center for Biomaterials and Biopathways, Zhejiang University, Hangzhou, Zhejiang 310027, China

Received August 9, 2006. In Final Form: February 15, 2007

An additive is not exclusively retardant or promoter for a crystallization system. The kinetic studies of calcium sulfate dihydrate (CSD) crystal growth demonstrated that borax played dual roles in the reaction, which accelerated CSD formations at the low concentration levels but inhibited the crystal growth at the high ones. In situ atomic force microscopy studies revealed that borax modulated the CSD crystallization via two different pathways: promoted the secondary nucleation to increase the step density on the growing crystal faces but simultaneously retarded the spread of these growth steps by the Langmuir adsorption. These two contradictory factors were incorporated in the crystallization, and their balance was regulated by the borax concentration. Both the macroscopic and microscopic experimental data nicely displayed the crystallization model of birth and spread that was able to account for the behaviors of borax in CSD formations.

Introduction

The modification effects of additives, or impurities, on crystallizations have been widely studied.[1−9] These growth modifiers can be organics, polymers, proteins, etc., but even small inorganic modifiers may play a role in these processes.[10−12] The additives affect the mechanisms of crystallization and aging processes, leading to the modification of formed crystal amounts, size distributions, habits, polymorphs, etc. The association of additives with crystallized structures and their observed effect on the crystal growth kinetics strongly suggest that additives modify the crystal growth stages.[13−15] However, many experimental results also suggest that additives control nucleation.[8−9,12,15−18] There is an inherent difficulty in studying the crystallization parameters as an isolated phenomenon, because all of them are intimately dependent in crystal formations. For an example, it is generally agreed that carboxylated compounds can lower the energy barrier and induce the precipitation of calcium salts, such as calcium oxalate and calcite, in the "modified" supersaturated solutions.[19−21] In contrast, it is also reported that the carboxyl-rich organic acids such as citrate can also dramatically retard the crystallization kinetic of calcium salts.[18] These different observations indicate that additives are not exclusively the inhibitors or promoters and their modification mechanisms are the subjects of extensive discussion.

Calcium sulfate dihydrate ($CaSO_4 \cdot 2H_2O$, CSD), gypsum, is of considerable importance since it is frequently encountered in nature and in industrial processes.[3,22] A variety of additives have been used to control the crystallization of CSD and hydrolysis of calcium sulfate hemihdydrate ($CaSO_4 \cdot 0.5H_2O$).[8−14,16,23] Borax (sodium borate, $Na_2B_4O_7$) is one of the extensively used regulators, and its retardant effect on CSD crystallization has been described.[24] Here, we study the influence of borax on the CSD crystallization at the macro- and nanoscales by using a constant composition method (CC) and atomic force microscopy (AFM), respectively. It is found that borax plays dual roles in CSD formation, which exhibits promotion and inhibition effects at the low and high concentrations, respectively. The characteristics of the crystallized CSD crystals are also altered accordingly with the change of borax concentration. A molecular modulation combined with the growth step kinetic is used to understand the mechanisms. The traditional birth and spread model which accounts for the dual roles of borax is experimentally observed and theoretically discussed. This study offers a general insight into the complexity and variety of the influences of modifying agents and gives a common idea on the kinetic control

* Corresponding author: e-mail, rtang@zju.edu.cn; tel/fax, + 86-571-87953736.

[†] Department of Chemistry.

[‡] Research Center for Biomaterials and Biopathways.

(1) Bujan, M.; Sikirić, M.; Filipović-Vinceković, N.; Vdović, N.; Garti, H.; Füredi-Milhofer, N. *Langmuir* **2001**, *17*, 6461.

(2) De Yoreo, J. J.; Dove, P. M. *Science* **2004**, *306*, 1301.

(3) Öner, M.; Doğan, Ö.; Öner, G. *J. Cryst. Growth* **1998**, *186*, 427.

(4) Elhadj, S. Salter, E. A.; Wierzbicki, A.; De Yoreo, J. J.; Han, N.; Dove; P. M. *Cryst. Growth Des.* **2006**, *6*, 197.

(5) Orme, C. A.; Noy, A.; Wierzbicki, A.; McBride, M. T.; Grantham, M.; Teng, H. H.; Dove, P. M.; DeYoreo, J. J. *Nature* **2001**, *411*, 775.

(6) Qiu, S. R.; Wierzbicki, A.; Orme, C. A.; Cody, A. M.; Hoyer, J. R.; Nancollas, G. H.; Zepeda, S.; De Yoreo, J. J. *Proc. Natl. Acad. Sci. U.S.A.* **2004**, *101*, 1811.

(7) Jung, T.; Sheng, X.; Choi, C. K.; Kim, W. S.; Wesson, J. A.; Ward, M. D. *Langmuir* **2004**, *20*, 8587.

(8) Prisciandaro, M.; Lancia, A.; Musmarra D. *Ind. Eng. Chem. Res.* **2003**, *42*, 6647.

(9) Prisciandaro, M.; Olivieri, E.; Lancia, A.; Musmarra, D. *Ind. Eng. Chem. Res.* **2006**, *45*, 2070.

(10) Rashad, M. M.; Mahmoud, M. H. H.; Ibrahim, I. A.; Abdel-Aal, E. A. *J. Cryst. Growth* **2004**, *267*, 372.

(11) Kruger, A.; Focke, W. W.; Kwela, Z.; Fowles, R. *Ind. Eng. Chem. Res.* **2001**, *40*, 1364.

(12) Prisciandaro, M.; Lancia, A.; Musmarra, D. *Ind. Eng. Chem. Res.* **2001**, *40*, 2335.

(13) El-Shall, H.; Rashad, M. M.; Abdel-Aal, E. A. *Cryst. Res. Technol.* **2005**, *40*, 860.

(14) Elisabeth Badens, Ste phane Veesler, Roland Boistelle. *J. Cryst. Growth* **1999**, *198/199*, 704.

(15) Davey, R. J. *J. Cryst. Growth* **1976**, *34*, 109.

(16) Mahmoud, M. H. H.; Rashad, M. M.; Ibrahim, I. A.; Abdel-Aal' E. A. *J. Colloid Interface Sci.* **2004**, *270*, 99.

(17) Birchall, J. D.; Davey, R. J. *J. Cryst. Growth* **1981**, *54*, 323.

(18) Tang, R, Darragh, M.; Orme, C. A.; Guan, X.; Hoyer, J. R.; Nancollas G. H. *Angew. Chem., Int. Ed.* **2005**, *44*, 3698.

(19) Mann, S.; Didymus, J. M.; Sanderson, N. P.; Heywood, B. R.; Samper, E. J. A. *J. Chem. Soc., Faraday. Trans.* **1990**, *86*, 1873.

(20) Mann, S.; Archibald, D. D.; Didymus, J. M.; Douglas, T.; Heywood, B. R.; Meldrum, F. C.; Reeves, N. J. *Science* **1993**, *261*, 1286.

(21) Mann, S.; Heywood, B. R.; Rajam, S.; Birchall, J. D. *Nature* **1988**, *334*, 692.

(22) Klepetsanis, P. G.; Dalas, E.; Koutsoukos P. G. *Langmuir* **1999**, *15*, 1534.

(23) El-Shall, H.; Rashad, M. M.; Abdel-Aal, E. A. *Cryst. Res. Technol.* **2002**, *37*, 1264.

(24) McCartney, E. R.; Alexander, A. E. *J. Colloid Sci.* **1958**, *13*, 383.

10.1021/la062366g CCC: $37.00
Published on Web 03/27/2007

of crystallization. Furthermore, this CSD−borax system is of particular interest not only for fundamental research but also for their importance in applications.

Materials and Methods

Constant Composition Method In the CC method, titrant solutions are used to maintain constant concentrations of the reaction solutions and kinetic growth results can be calculated from the rates of titrant addition. Crystallization experiments were made in magnetically stirred (450 rpm) double-walled Pyrex vessels at a temperature of 25.0 ± 0.1 °C. The supersaturated reaction solutions (200 mL) were prepared by mixing filtered (0.22 μm Millipore) calcium chloride and sodium sulfate stock solutions with sodium chloride to maintain the ionic strength, *I*, 0.40 M. The pH was adjusted to the desired value, 7.00 ± 0.01, using 0.1 M sodium hydroxide or sulfuric acid solution. Nitrogen, presaturated with water vapor at 25 °C, was purged through the reaction solutions to exclude carbon dioxide. Borax solutions were added prior to pH adjustments. The crystallization reactions were initiated by the introduction of 40.0 mg of CSD seed crystallites (the specific surface area, A_S, was 0.37 m^2/g, BET nitrogen adsorption: 30/70 N_2/He, Quantasorb II, Quantachrome Corp., Greenvale, NY). Titrant addition was potentiometrically controlled by calcium ion specific (Orion 93-20) and Ag/AgCl reference electrodes (Orion 900100). The calibrations of the calcium electrode in the absence and presence of borax were shown in the Supporting Information (Figure S1), which confirmed that borax did not reduce the sensitivity of the calcium electrode. During crystallization, the electrode potential was constantly compared with a preset value and the difference, or error signal, activated two motor-driven titrant burets to maintain a constant thermodynamic driving force. Concentrations of the titrant solutions which were used to compensate reaction solutions for growth were given by the following equations

$$T_{\text{calcium}} = 2W_{\text{calcium}} + C_e \quad \text{and} \quad T_{\text{NaCl}} = 2W_{\text{NaCl}} - 2C_e \qquad (1)$$

$$T_{\text{sulfate}} = 2W_{\text{sulfate}} + C_e \qquad (2)$$

where *W* and *T* were the total concentrations of the components in the reaction solution and the titrants, respectively. C_e stands for the effective titrant concentration (i.e., number of moles of CSD grown per liter of mixed titrants) and a value of 0.1 M was used in the experiments.

In the CC nucleation examinations, the experimental processes were similar to those of the seeded CC crystallization, but no CSD was added into the supersaturated solutions.

It should be mentioned that the calcium electrode could be stable in the solution during the experiment period. The calcium electrode in 0.01 M calcium chloride solution was checked before and after the CC experiments. During the CC experiment, solution samples were periodically withdrawn and filtered (0.22 μm Millpore filter) for the chemical analysis. The concentrations of calcium were also examined by using an atomic absorption method, which showed that the solution compositions remained constant to within 1.5% during the whole experiments.

Solution Speciation and Supersaturation The supersaturation, *S*, and relative supersaturation, σ, were given by

$$\sigma = S - 1 = \left[\frac{IP}{K_{sp}}\right]^{1/2} - 1 = \left[\frac{\alpha_{Ca^{2+}}\alpha_{SO_4^{2-}}}{K_{sp}}\right]^{1/2} - 1 \qquad (3)$$

in which α was the ionic activity of the ions or molecules and IP was the ionic activity product. The solubility activity product, K_{sp}, was 4.23×10^{-5} M^2.[25] Solution speciation calculations were made using the extended Debye−Hückel equation proposed by Davies from mass balance expressions for total calcium and total sulfate with appropriate equilibrium constants by successive approximation for the ionic strength.[26]

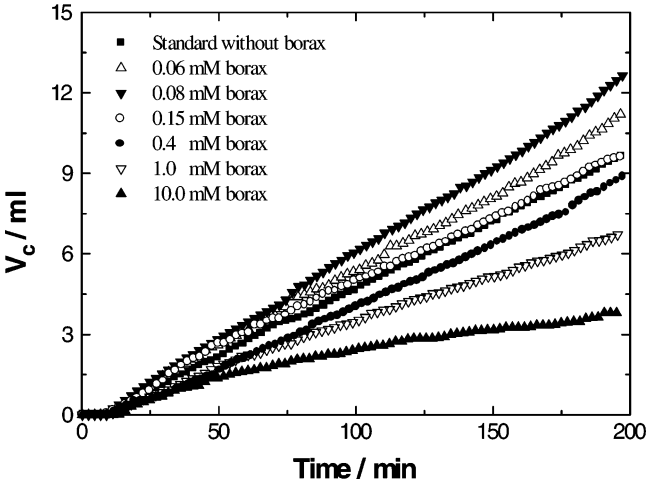

Figure 1. Plots of corrected titrant volume (V_c) against time in the absence and presence of borax for constant composition experiments ($\sigma = 0.33$).

In Situ Atomic Force Microscopy. AFM images were collected in contact mode by using a Veeco Multiple SPM with Nanoscope IVa controller. All images were acquired using the lowest tip force possible to reduce the tip−surface interaction. The CSD seed crystal was anchored inside the fluid cell, and the supersaturated solutions (identical to the CC studies) were passed through at 0.10 mL min^{-1} while the images were taken.

Scanning Electron Microscopy. Samples, under vacuum, were sputter-coated with a thin carbon deposit to provide conductivity and then examined using a field-emission scanning electron microscope (Hitachi S-4000), typically at 20 or 30 keV.

Simulation of the CSD−Borax Interface The molecular dynamics simulations were performed using the GROMACS package.[27,28] Periodic boundary conditions were applied in all directions. PME summation was applied for the long-range Coulomb interactions.[29,30] Our simulations were done in the *NpT* ensemble at atmospheric pressure and temperature of 298 K. The time step in the simulation was 2 fs. The force field parameter for CSD was provided by Adam.[31] The rigid SPC force fields,[32] widely used in modeling of aqueous systems, were applied for water. The van der Waal interaction force field parameter of boron was taken from MM2 force field.[33] And the bond force field parameter of borate anion and boric acid were calculated by quantum mechanic calculation with the B3LYP method, and the partial charges of each atom were calculated by the CHELPG method.

Results and Discussion

The results in Figure 1 were expressed as plots of correct volume, V_c, against time, *t*, in which V_c was calculated from *V*, the original volumes of titrant addation in the CC experiments,

(25) Marshall, W. L.; Slusher, R. *J. Phys. Chem.* **1966**, *70*, 4015.

(26) Davies, C. W. *Ion Association*; Butterworths: London, 1962.

(27) Berendsen, H. J. C.; van der Spoel, D.; van Drunen, R. *Comp. Phys. Commun.* **1995**, *91*, 43.

(28) Lindahl, E.; Hess, B.; van der Spoel, D. *J. Mol. Mod.* **2001**, *7*, 306.

(29) Darden, T.; York, D.; Pedersen, L. *J. Chem. Phys.* **1993**, *98*, 10089.

(30) Essmann, U.; Perera, L.; Berkowitz, M. L.; Darden, T.; Lee, H.; Pedersen, L. G. *J. Chem. Phys.* **1995**, *103*, 8577.

(31) Adam, C. D. *J. Solid State Chem.* **2003**, *174*, 141.

(32) Berendsen, H. J. C.; Postma, J. P. M.; van Gunsteren, W. F.; Hermans, J. Interaction models for water in relation to protein hydration. In: *Intermolecular Forces*; Pullman, B., Ed.; D. Reidel Publishing Co.: Dordrecht, 1981; pp 331−342.

(33) Allinger, N. L. *J. Am. Chem. Soc.* **1977**, *99*, 8127.

by eq 4[34]

$$V_c = \frac{(1 + MC_eV/m_0)^{1-p} - 1}{(1-p)MC_e/m_0} \quad (4)$$

where M was the molecular mass of CSD, m_0 the initial mass of the CSD seed crystallites, and p a growth correction factor, which was experimentally determined previously in our laboratory to be approximately 0.4. V_c was used to take into account the increasing mass of CSD crystallites during the CC crystallization experiments. After the application of corrections of titrant volumes, relatively linear plots were obtained for the CC crystallizations and the rates of the reactions could be determined by eq 5

$$R = \frac{C_e d}{m_0 A_s} \quad (5)$$

in which R (i.e., the molar of CSD increases per surface area per min) was the crystallization rate, d the slopes of V_c-t plots in Figure 1, and A_s the specific surface area of CSD seed.

In Figure 1, the relative supersaturation of reaction solution, σ, was 0.33 (the final concentrations of calcium and sulfate were 0.04089 M). Under this condition, the normalized CSD crystallization rate in the absence of borax was 0.303 mmol m^{-2} min^{-1}. Borax could dramatically modify the kinetics of CSD crystallization and had the dual behaviors, which accelerated the CSD crystallizations at low concentration level but inhibited the reaction at high concentrations. Within the borax concentration of 0.08 mM, the CSD CC rate increased with the increasing of borax and reached a maximum value of 0.414 mmol m^{-2} min^{-1}, 36% higher than the control one. However, this acceleration tendency was not sustained with further increase of borax, and the crystallization rate began to drop when the borax concentration was higher than 0.08 mM. The rates decreased to 0.313 and 0.224 mmol m^{-2} min^{-1} at borax concentrations of 0.15 and 1.0 mM, respectively. In the presence of 10 mM borax, the CSD crystallization rate was only 0.127 mmol m^{-2} min^{-1}, lower by about 70% compared with the fastest one at 0.08 mM. It was emphasized that since the ratios of borax to calcium could be negligible in most experimental conditions, changes in calcium concentration due to the formation of calcium borax complexes could be ruled out. Thus, the modification on the thermodynamic driving force for crystallization was not a key factor.

The dual effects of borax on CSD crystallization were also observed under the different experimental conditions ($\sigma = 0.14$, 0.24, and 0.48) by using the CC method (Figure S2). In order to find the mechanism of the dual effects, the $\sigma = 0.33$ was selected for in-depth investigation, which could meet the requirements of both CC and AFM studies simultaneously.

It is well-known that a crystallization process includes at least two processes: nucleation (i.e., 2D nucleation onto an existing crystal surface and 3D nucleation in bulk solution) and crystal growth (i.e., step movement)[35−37] Under the in situ AFM, it could be noted that the CSD (010) crystal surfaces consisted of flat regions called terraces and raised partial layers called steps (Figure 2) in the supersaturated solutions. The step heights were around 0.75 nm, one-half of the lattice parameter along the b axis of CSD, 1.520 nm. In the solutions, the step edges were not static; molecules were constantly attaching and detaching. Growth from a supersaturated solution occurred because the flux of molecules attaching to the crystal surface exceeded the flux of molecules detaching from the surface, and therefore, the steps could move forward, resulting in the crystal growth. The spread rates of these steps were usually proportional to the bulk crystal growth rates in most crystallization cases. In situ AFM experiments, made under the same conditions as those for the CC studies, showed that borax could only reduce the step velocities in the whole borax level of 0−10 mM. It can be seen in Figure 3a that with an increasing of the borax concentration, the step velocities of CSD on the (010) growing surfaces, V_{step}, kept on dropping. The average step movement rates ($n \geq 50$) were 13.1, 12.9, 10.4, 6.7, and 4.8 nm s^{-1} at the borax concentrations of 0, 0.06, 0.15, 0.6, and 1.0 mM, respectively. The effectiveness of borax as a growth inhibitor suggested adsorption of the molecules on the crystal surfaces or steps. When impurities adsorbed onto the steps, they could block the advancement of

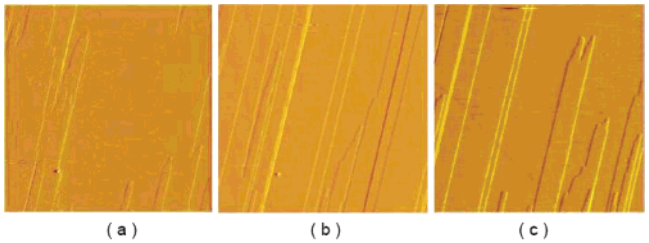

Figure 2. AFM frames of the CSD growing (010) crystal faces at $C_{borax} = 0$ (a), 0.08 (b) and 1.0 mM (c). The image scales are 5×5 μm.

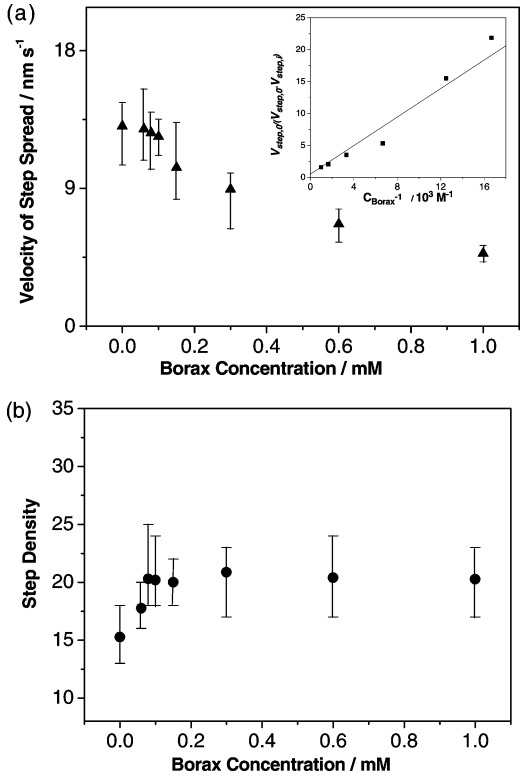

Figure 3. Step spread on the (010) CSD surfaces was inhibited by the increasing of borax concentrations (a), the inserted plot shows the "Langmuir" kinetic adsorption isotherm for the influence of borax on the CSD step movements; in contrast, borax could increase the step density (step amount per 5×5 μm frame) on the growing crystal face (b).

(34) Zhang, J.; Nancollas, G. H. *J. Cryst. Growth* **1992**, *118*, 287.
(35) Burton, W. K.; Cabrera, N.; Frank, F. C. *Philos. Trans. R. Soc. London* **1951**, *A243*, 299.
(36) Hurle, D. T. J. *Handbook of Crystal Growth*; North-Holland: Amsterdam−London−New York−Tokyo, 1993.
(37) De Yoreo, J. J.; Vekilov, P. Principles of crystal nucleation and growth. In *Biomineralization*; Dove, P. M., De Yoreo, J. J., Weiner, S., Eds.; Mineral Society of Ammerica: Washington, DC, 2003; pp 57−93.

the steps at that site. This adsorption of inhibitor molecules might be interpreted in terms of a Langmuir equilibrium adsorption isotherm. The application of this model in interpreting the reduction in the crystal growth in the presence of inhibitors has been very successful.[38,39] In terms of the crystal growth rate, the Langmuir adsorption isotherm may be written as eq 6

$$\frac{V_0 - V_i}{V_0} = \frac{1}{1-b} + \frac{1}{(1-b)KC} \quad (6)$$

where V_0 and V_i are the crystal growth rates (or the step movement rates) in the absence and in the presence of inhibitor, respectively, and b is a dimensionless parameter, K, adsorption affinity constant of inhibitor onto the crystal surfaces. If $b = 0$, the inhibitor is capable of completely inhibiting the growth at concentrations approaching infinity. The inhibitor is incapable of completely inhibiting crystal growth if $0 < b < 1$, while if $b < 0$, the inhibitor can completely suppress the reaction at concentrations below those corresponding to a monolayer. The insert in Figure 3a shows that the step spread of CSD in the presence of borax could fit this Langmuir kinetic adsorption model well. However, such a relationship could not be established in the CC bulk studies. Values of $K = 353 \pm 24$ and $b = -1.16 \pm 0.07$ were obtained from the linear plot of $V_{step,0}/(V_{step,0} - V_{step,i})$ as a function of C_{borax}^{-1}. It was also an example to show that the adsorption constant of molecules or ions onto a crystal face or step could be studied at the nanoscale by using AFM.

Clearly, borax had the inhibition effect on the step movements, which should imply that it was an inhibitor of CSD crystal growth. However, the value of K was relatively low in comparison with other additives, indicating that borax was not an excellent inhibitor. It was consistent with the CC experiments as that the significant inhibition effect of borax was only observed under the high concentrations (Figure 1). We also used the Langmuir model to fit a part of CC data with high borax concentrations (0.4, 1.0, and 10 mM, since the significant inhibition effect was observed under these conditions) and the estimated K was around 280 (Figure S3). And this value from the bulk study was similar to that from step measurements on the (010) face, their difference would be explained later.

However, the conclusion of inhibition effect of borax was not consistent completely with all the CC phenomena as the crystallization was accelerated at a low concentration level (<0.1 mM). Besides the step velocity, it was well-known that the step density was another important factor, which could determine the kinetics of crystallizations too. Figure 2 and Figure 3b show that in the presence of various concentrations of borax, the step density growing (010) CSD faces was significantly greater than the control one. More than 30 AFM frames under each experimental condition were collected, the steps were accounted for, and their average statistical value was considered as the step density (i.e., amount of steps per frame), N_{step}. In the presence of borax, the step density was always greater than the control. It was noted that only a small amount (within 0.1 mM) of borax could greatly increase the step density and the values of N_{step} remained at a relatively constant value with further increase of the borax concentration (Figure 3b). Interestingly, this AFM study on the step density indicated that borax was a crystallization promoter, which was against the conclusion from the step movement measurements. Thus, we could also explain that the K value from CC was a little bit smaller than that from the AFM step measurement since, in the Langmuir inhibition fit of CC kinetic data, this promotion effect was not excluded in the calculations.

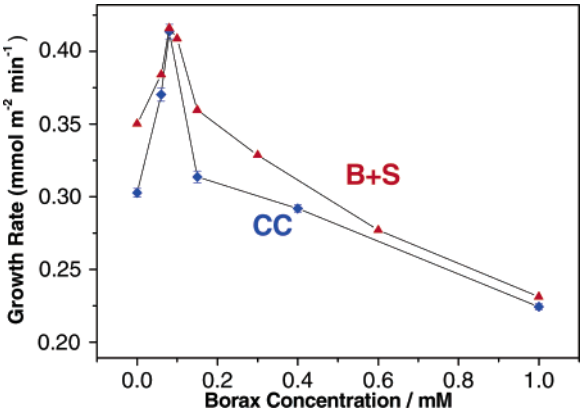

Figure 4. Curves of calculated CSD crystallization rates using B+S model and the experimental CC crystallization rates.

These two contradicted factors could be incorporated by using a classical birth-and-spread (B+S) model for crystallization,[36] the bulk crystallization rate, R, could be expressed by step spread velocity, V_{step}, and nucleation rate, J_N

$$R = \alpha V_{step}^{2/3} J_N^{1/3} \quad (7)$$

where α was a constant. R was a function of V_{step} and J_N. The experimental results indicated V_{step} of CSD decreased while J_N increased simultaneously with the presence of borax. Since N_{step} was related to J_N,[8] N_{step} could be used to simplify the discussion. Figure 4 showed the calculated crystallization rates by eq 7 together with the measured CC rates at various borax concentrations. The two curves (theoretical and experimental) had the similar behaviors to demonstrate the dual effects of borax on the CSD formations.

From Figure 3 it could be seen that the nucleation promotion (or step density increase) effect was even remarked at the low concentration levels of borax and then approached a relative constant when $C_{borax} > 0.08$ mM. In contrast, the inhibition effects on the step movement kept on increasing with an increase of borax concentrations. When borax concentration was lower than 0.08 mM, the decrease of the V_{step} could be neglected and the acceleration of N_{step} dominated the change of R. In this stage, the influence of borax on the nucleation rates was much more sensitive than the inhibition of step movements. Although the nucleation was still promoted in the borax levels of 0.08−0.2 mM, the inhibition effects of borax on the step movements were more significant and R began to drop despite the high nucleation rates. At the concentrations of >0.2 mM, N_{step} remained almost unchanged but V_{step} dropped greatly, the reduction of step velocity began to dominate in the reaction and the promotion effect of nucleation was fully counteracted, resulting in the significant crystallization inhibitions. The mismatch of the two curves in Figure 4 might be caused by the calculations only showing the crystallization modification on the (010) CSD faces but the CC results reflected the crystallization kinetics of all CSD faces. However, it was important to note that the dual roles of borax in CSD crystallizations were confirmed by using the B+S model at the macroscopic and microscopic scales.

These dual effects were also confirmed by the CC nucleation study (Figure 5). It is well-known that the spontaneous crystallization does not occur in the supersaturated solution until the driving force (supersaturation) is sufficiently high or seed crystals are added. Rather, a metastable equilibrium condition persists

(38) Nancollas, G. H.; Zawacki, S. J. In *Industrial Crystallization '84*; Jancic, S. J., DeLong, E. J., Eds.; Elsevier: Amsterdam, 1984.
(39) Tang, R.; Wu, W.; Hass, M.; Nancollas, G. H. *Langmuir* **2001**, *17*, 3480.

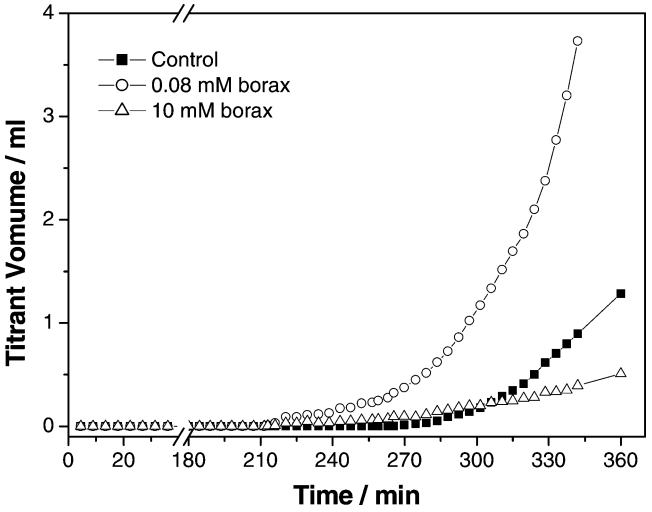

Figure 5. Plots of titrant volume (*V*, the volume was not corrected) against time in the absence and presence of borax in the constant composition nucleation experiments.

during an "induction period", τ, prior to crystal nucleation. At σ of 0.33, the CSD supersaturated solution could be metastable for around 250 min. An introduction of borax into this nucleation experiment could reduce the induction time obviously, indicating the promotion effect of CSD nucleation. In the presence of 0.08 mM borax, τ was decreased to 200 min. However, the further increasing of borax concentration could not affect the values of τ any more. Even at the highest concentrations of borax, 10 mM, the nucleation also occurred at ~200 min. As we mentioned, the step density was somehow related to the nucleation reaction, J_N. Since $\tau \propto 1/J_N$, these results from the macroscopic CC nucleation experiments fitted with the findings from microscopic AFM examinations well. As an expectation, the crystallization rate of CSD in the presence of 0.08 mM was greater than the control, which was obtained from the slopes of curves in Figure 5 (a larger slope indicated a faster crystallization rate). Although 10 mM borax could induce the nucleation, the subsequent crystallization was significantly inhibited. These CC nucleation results were in good agreement with the observations in the AFM and CC seeded crystallizations. Again, the two contradicting effects of borax on CSD formation, promotion effect on nucleation and inhibition effect on crystal growth, were demonstrated simultaneously and clearly.

Since the nucleation of CSD was promoted by borax, the formations of the new nuclei in the supersaturated CSD solution should be observed accordingly. As a result, although the CC rates of CSD in the presence of 0.08 mM borax were faster than the control, the resulting crystal sizes were not larger (Figure 6). Numerous small crystals were observed under scanning electron microscopy (SEM), which could account for the newly nucleated crystallites in the supersaturated solutions. Since the secondary nucleations of CSD in the supersaturated solutions dominated the crystallization, therefore, the obtained crystals always had irregular morphologies and rough surfaces in the presence of 0.08 mM borax. In the presence of 10 mM borax, the grown CSD by CC method had the analogous morphologies to those of the control. Their crystal sizes were much smaller, which represented a typical effect of the growth inhibition. Meanwhile, the formation of numerous small crystallites was also detected widely on the SEM image. Furthermore, the size distribution studies (Malvern Particle Sizer 3600E) could give the overall views of the obtained particles, which also confirmed the dual effect of borax during the CC experiments. Since the length of original CSD seed was ca. 50−80 μm, the appearance of the band of 10−40 μm in Figure 6f could be attributed to the newly formed CSD in the bulk solutions. This band could be ignored in the control experiment, but it was enhanced significantly by the presence of borax. Meanwhile, the average crystal sizes decreased with the increasing of borax concentration. For example, at a borax concentraion of 10 mM, the main peak was shifted from ca. 85 μm (control) to ca. 70 μm, but the band of 10−40 μm increased about three times more than the control. These experimental results clearly implied that the crystal growth of CSD was retarded but the induced nucleation (forming new crystallites) was promoted by borax. It should be mentioned that even at such a high concentration of borax, the element of boron was not detected on the resulted CSD by using energy dispersive spectroscopy (EDS, Figure 6e). Together with the results of X-ray diffraction (Figures S4 and S5), it was concluded that the direct precipitation of calcium borate did not occur and boron did not incorporate into the CSD crystallites during the modified reactions. This phenomenon was also in agreement of the weak interaction between borate and CSD. It should be noted that in the presence of 0.40 mM borax, most of the obtained CSD crystallines were needlelike. This indicated the anisotopic kinetics modifications by borax on the different CSD faces, which would be studied and discussed elsewhere.

One of the major challenges in crystal growth science today is to understand the physical mechanisms by which this level of control is achieved. A very general and useful construct for thinking about the problem is the energy landscape.[18,37] All aspects of a crystal, including its phase, habit, and growth rate, are determined by the shape of the landscape. Equilibrium crystal habit and phase are controlled by the depths and shapes of the energy minima. By varying the heights of the barriers, the growth kinetics can be controlled, and nonequilibrium final or intermediate states can be selected. It stood to reason that the additives such as borax modulated crystal growth by manipulating the energy landscapes. A complete physical picture of the modification effects required a description of the geometry and stereochemistry of the interaction between the CSD crystal lattice and borax, the magnitude of the interaction energy, the effect of that interaction on the energy landscape, and the impact of the change in the landscape on crystallization. Recently, we have suggested that such modifications could result from the solid−solution interfacial energies.[18] Under our experimental conditions, the species of $B(OH)_4^-$ and $B(OH)_3$ were the main speciation in the solutions. With computer simulations, it was revealed that $B(OH)_4^-$ ions could bind to the calcium-rich sites (Figure 7, labeled as 1) or with the structured water molecules (labeled as 2) on the crystal surfaces. Some of $B(OH)_3$ molecules adsorbed onto the immobile water layer (labeled as 3) but the rest remained in the bulk solutions (labeled as 4). Only a part of borate adsorbed onto the CSD surfaces, and this phenomenon also indicated the relatively low affinity of borax on CSD. However, the adsorbed ions and molecules could change the CSD−solution interfacial properties. The largest crystal face, (010) of CSD was used for this estimation. In the pure CSD−water system, the calculated interfacial energy, γ, was 0.451 J m^{-2}. When the borax was added, the CSD−solution interfacial energy decreased to 0.434 J m^{-2}, and this value was almost independent upon the borax concentration in the range of 0.1−1.0 mM, in agreement with the experimental phenomena of the step density (Figure 3b). As the descriptions of the interfacial control model,[18] the low values of interfacial energy indicated a low-energy barrier for nucleation. Therefore, the three-dimensional (3-D) nucleations in the solution

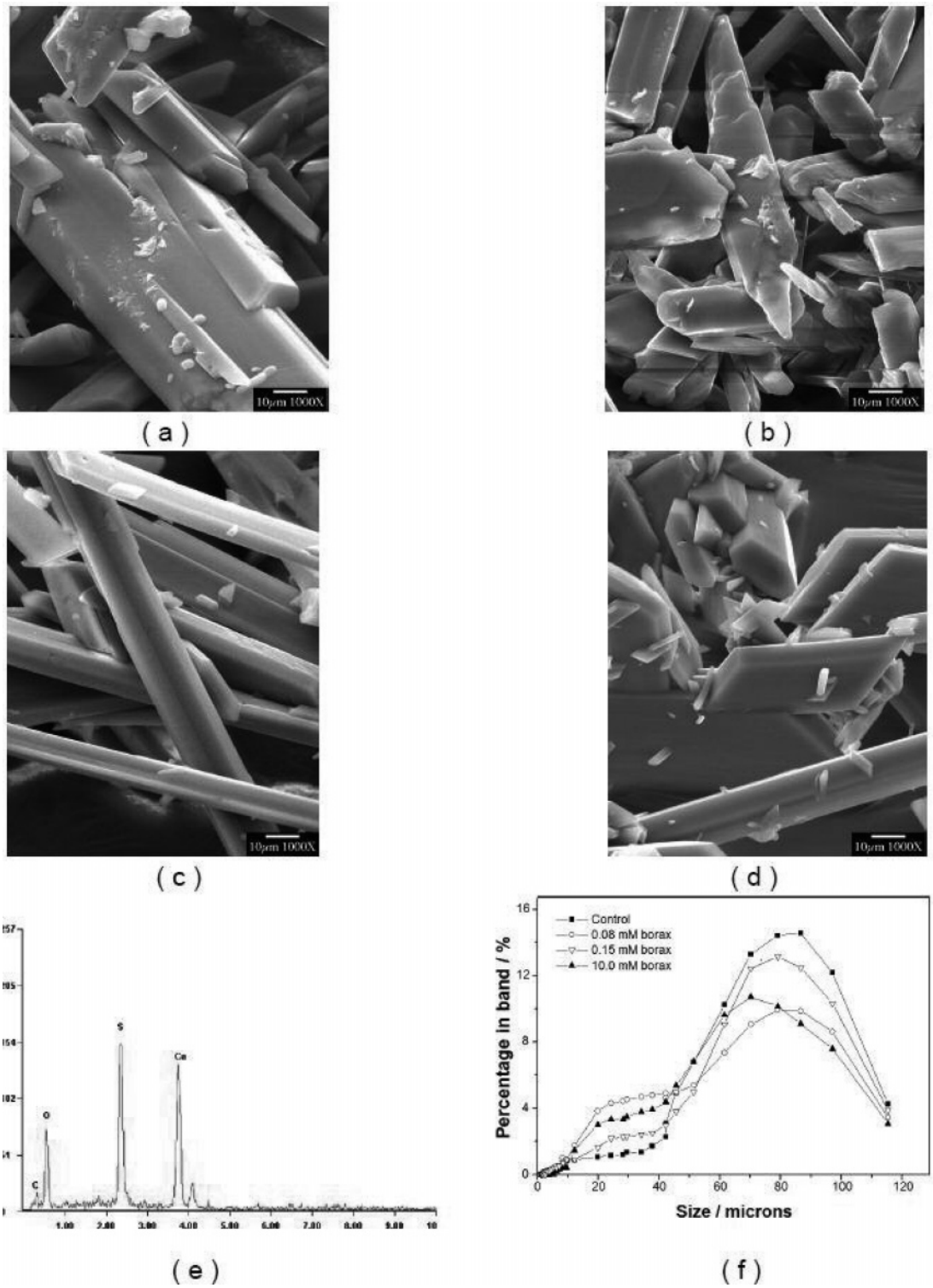

Figure 6. SEM mircrographs of the grown CSD in the presence of 0 (a), 0.08 (b), 0.40 (c), and 10.0 mM (d) borax. (e) EDS pattern of the resulting crystallites in the presence of 10 mM borax, the element carbon was from the substrate. (f) Particle size distribution of crystallized CSD in the solution in the absence and presence of borax.

or 2-D nucleations on the existing CSD surfaces were promoted as a description of eq 8

$$\ln J_N = \alpha_1 + \alpha_2 \frac{k^3 T^3 (\ln S)^2}{\gamma^3} \qquad (8)$$

where, k is the Boltzmann constant, T is the absolute temperature, α_1 and α_2 are the kinetic constants. This equation shows that nucleation rate, J_N, is increased with a decreasing of interfacial energy. Accordingly, the induction time, τ, should be decreased and more steps should form on the growing crystal faces with the introduction of borax, which were observed experimentally by CC and AFM, respectively. Although the detailed relationship between τ and γ was not examined in this study, the tendency of the decreasing effect of interfacial energies of CSD−solution by the borax was already shown theoretically and experimentally.

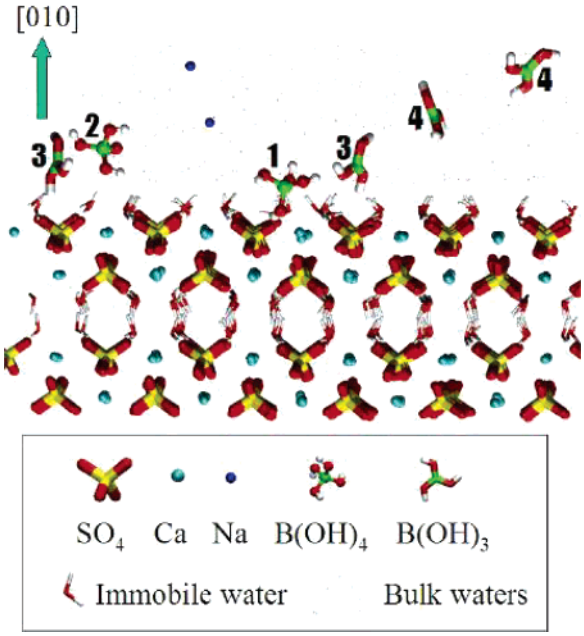

Figure 7. Simulation of adsorptions of borate at the (010) CSD−water interface.

It also showed that the molecular simulation could be another useful tool for an understanding of interfacial phenomena in the crystal modification. Both macro- and microscale studies showed that the crystallization kinetics of CSD were controlled by the borax concentrations and tracked the description of the B+S model.

Conclusion

By using the macroscopic (CC seeded crystallization, CC nucleation, XRD, and size distribution measurement) and microscopic (AFM, SEM, and EDS) methods, we have concluded that the behaviors of borax in the CSD crystallization system are in excellent agreement with the predictions of the B+S model. The results of CC nucleation and computer simulation show that borax can reduce the interfacial energy of the CSD−solution to promote the nucleation, which was also detected by using AFM. However, the adsorption of borax onto a CSD surface can block the attachment of calcium and sulfate to retard the step spread. The balance of the two contradictory effects is regulated by the additive concentrations. The nucleation promotion and the inhibition of step growth dominate the crystallizations at the low and high concentration levels, respectively. The kinetics data are well matched by the B+S model and Langmuir kinetic adsorption model. These results clearly demonstrate that additives do not actually possess an absolute characterization such as retardants or promoters, which can be regulated by the experimental circumstances.

Acknowledgment. We thank Drs. George H. Nancollas, Ali Hina, and Tao Wu for their helpful discussions. This work was supported by National Natural Science Foundation of China (20571064), Changjiang Scholars Program (R.T.), and Zhejiang University.

Supporting Information Available: Figures showing calibrations of the Orion 90-20 calcium electrode in the presence and absence of borax, plots of corrected titrant volume against time in the absence and presence of borax, the Langmuir kinetic adsorption isotherm for the influence of borax on the CC crystallization of CSD in the presence of 0.4, 1.0, and 10 mM borax, and XRD spectra of the precipitated crystallites in the absence and presence of borax. This material is available free of charge via the Internet at http://pubs.acs.org.

LA062366G